International Journal of Pharmaceutics 404 (2011) 317–323

Contents lists available at ScienceDirect

International Journal of Pharmaceutics

journal homepage: www.elsevier.com/locate/ijpharm

Pharmaceutical Nanotechnology

Preparation of new 5-fluorouracil-loaded zein nanoparticles for liver targeting

L.F. Lai, H.X. Guo*

Department of Pharmaceutics, Faculty of Pharmacy, Shandong University, 250012 Jinan, China

ARTICLE INFO

Article history:
Received 25 August 2010
Received in revised form 6 October 2010
Accepted 12 November 2010
Available online 19 November 2010

Keywords:
Zein nanoparticles
5-FU
Encapsulation
Uniform experimental design
Liver targeting

ABSTRACT

This study proposes a new zein nanoparticle (ZP) encapsulated 5-fluorouracil (5-FU) that target liver through intravenous delivery. The ZPs were prepared by phase separation process and optimized using uniform experimental design. The physical properties, in vitro drug release and stability of optimal drug-loaded ZPs were studied. The biodistribution and the target efficiency of the particles were investigated in a mouse model. The highest drug loading was obtained using zein: 5-FU, 3:1 (v/v); zein concentration, 12.5 mg/ml, pH 9.18, mixing time, 3 h and ethanol concentration, 40%. The encapsulation efficiency and the drug loading were 60.7 ± 1.74 and 9.17 ± 0.11 respectively. The size of ZPs and zeta potential were 114.9 ± 59.4 nm and -45 ± 0.3 mV respectively. Differential scanning calorimetry (DSC) demonstrated that the drug was encapsulated within the ZPs. A sustained release profile of 5-FU was observed from ZPs. The more stable storage condition of ZPs was at a temperature of 4 °C. In vivo, ZPs was mostly accumulated in liver following intravenous injection, and the targeting efficiency increased 31.33%. The relative uptake rate of liver was 2.79. Also, nano-sized ZPs were beneficial for prolonged blood residence (7.2-fold increase). These demonstrated that the drug-loaded ZPs could be efficiently targeted at the liver by intravenous delivery.

1. Introduction

Biodegradable nanoparticles (NPs) are receiving considerable attention for the delivery of therapeutic drugs. The literature emphasizes the advantages of nanoparticles over microparticles (McClean et al., 1998) and liposomes (Soppimath et al., 2001). The submicron size of nanoparticles offers a number of distinct advantages over microparticles, including relatively higher intracellular uptake compared to microparticles. To target tumor cells more selectively, active targeting based on antibodies or receptor mediated targeting with cancer specific ligands are developed. However, recent clinical results of molecular target based drugs have shown somewhat disappointing results due to inherent heterogeneity and epitopic diversification of tumor cells even amongst the same cancer patient (Tobias et al., 2006; Greenman et al., 2007). Furthermore, the efficacy of molecular target drugs exhibited only a 4–5% response rate despite of very high expectation and very high cost of manufacturing (Maeda et al., 2009).

NPs may be delivered to specific sites by size-dependant passive targeting (Matsumura and Maeda, 1986). Passive delivery refers to NP transport through leaky tumor capillary fenestrations into the tumor interstitium and cells by passive diffusion or convection (Yuan, 1998). Nanoparticles ranging from 10 to 100 nm in size then begin to accumulate within tumors because of their ineffective lymphatic drainage. This is a phenomenon known as the enhanced permeability and retention (EPR) effect (Teicher, 2000; Sledge and Miller, 2003). Passive targeting can result in increases in drug concentrations in solid tumors of several-folds relative to those obtained with free drugs (Moghimi et al., 2001). Recently, Maeda et al. (2009) highlighted that polymeric drugs for efficient tumor targeted drug delivery were based on EPR-effect. The EPR effect can be observed in almost all human cancers with the exception of hypovascular tumors like prostate cancer or pancreatic cancer. For such a passive targeting mechanism to work, the size of the nanoparticles must be controlled to avoid uptake by the reticuloendothelial system (RES) (Gref et al., 1994). The nanoparticles injected intravenously are mainly delivered to the mononuclear phagocytes system (MPS) (liver, spleen, lungs and bone marrow). Both the polymeric compositions (type, hydrophobicity and biodegradation profile) of the nanoparticles and the associated drug (molecular weight, charge, localization in the nanospheres: adsorbed or incorporated) have a great influence on the drug distribution pattern in the reticuloendothelial organs (Couvreur et al., 1980). This effect was rapid (within 0.5 or 3 h) and compatible with endocytosis. Such propensity of MPS macrophages for endocytosis/phagocytosis provides an opportunity to efficiently deliver therapeutic agents to these cells, using un-modified nanoparticles. This biodistribution can be of benefit for the chemotherapeutic treatment of MPS localized tumors (for example, hepatocarcinoma or hepatic metastasis arising from digestive tract or gynaecological cancers).

* Corresponding author. Tel.: +86 531 88382007; fax: +86 531 88382548.
E-mail addresses: hongxiaguo@sdu.edu.cn, hongxia.guo@gmail.com (H.X. Guo).

0378-5173/$ – see front matter © 2010 Published by Elsevier B.V.
doi:10.1016/j.ijpharm.2010.11.025

Biodegradable polymers such as PLGA have been extensively studied in controlled release technology. However, it had some limitations for the encapsulation sensitive therapeutic agents during bulk erosion (Park et al., 1995). Depending on the physicochemical characteristics of a drug, it is possible to choose the best polymer to achieve an efficient entrapment of the drug. Zein is an alcohol soluble protein of corn origin that exhibits hydrophobic properties. Zein showed a good biocompatibility for the development of tissue engineering (Dong et al., 2004). It has been studied as microparticle drug delivery system (Liu et al., 2005). In aqueous ethanol solution zein exists as small globules with diameters between 150 and 550 nm (Guo et al., 2005). The zein molecular has a very special bricklike shape and thus has a potential to carry other molecular inside them. In order to exhibit features of the EPR effect, a drug must have a higher molecular weight than the renal excretion threshold (typically >40 kDa) (Matsumura and Maeda, 1986; Maeda et al., 2001; Noguchi et al., 1998; Seymour et al., 1994). Zein has a molecular weight of about 40 kDa. It is a natural protein and has a good biodegradability in vivo (Wang et al., 2007). Zein and its degraded product showed good cell compatibility (Dong et al., 2004; Liu et al., 2005; Wang et al., 2005). It has the advantages vs. synthetic nanomaterials for its absorbability and for the low toxicity of the degradation end products (Liu et al., 2005). It can also overcome the drawback of hydrophilic polymeric system in order to achieve sustained drug release. These are the basis for further study. Until now, there is no study related to drug-loaded ZPs for liver targeting.

5-Fluorouracil (5-FU) has a long history of use as a chemotherapeutic agent. However, less than 20% of an injected dose undergoes enzymatic activation (Tanaka et al., 2000). The oral bioavailability of 5-FU is unpredictable due to high variability in enzymatic degradation (Grem, 1990). With the typical dose of 600 mg/m^2/day, tumor cells are only exposed to the rate-limited active metabolites for a brief time. This is due to the short half-life of 5-FU locally within tissues as well as systemically ($t_{1/2}$ = 10–20 min) (Tanaka et al., 2000). Furthermore, a problem with 5-FU therapy is its toxicity to the bone marrow and the gastrointestinal tract. It has been recognized that, optimally, this drug should be dosed once or twice a week, preferably as a long-acting injection and targeted to the desired site. Biodegradable microparticle delivery system is one promising way for achieving this (Zan et al., 2006; Lamprecht et al., 2003).

In the present study, 5-FU-loaded ZPs were prepared and optimized using uniform experimental design for liver targeting. The physical properties, stability and the in vitro release of 5-FU-loaded ZPs were investigated. Additionally, biodistribution and target efficiency of the prepared ZPs were studied in vivo in normal mice.

2. Materials and methods

2.1. Materials

The following materials and chemicals were obtained from commercial suppliers: zein (Bache Pharmaceutical Co., Wujiang, China), 5-FU (Qilu Pharmaceutical Co., Shandong, China), ethanol (Yongda Chemical Co., Tianjin, China), methanol (Guangcheng chemical Co., Tianjin, China) and rhodamine B (Sigma).

2.2. Preparation of zein nanoparticles

5-FU-loaded zein nanoparticles were prepared using a phase separation procedure. Typically certain proportional 5-FU and zein were dissolved in 5 ml 70% ethanol (w/w) ultrasonically. The resulting solution was immediately added in 9 ml distilled water. The formed dispersion was allowed to evaporate at room temperature to harden the particles. The dispersion was centrifuged, washed three times with ethyl acetate and freeze-dried.

Table 1
The levels and factors of uniform experimental design.

Levels	Factors				
	X_1 (v/v)	X_2 (mg/ml)	X_3	X_4 (h)	X_5 (%)
1	16:1	2.5	3.0	1	25
2	12:1	5	4.0	2	30
3	8:1	7.5	5.8	3	35
4	4:1	10	7.8	4	40
5	2:1	12.5	9.18	5	45

2.3. Drug encapsulation efficiency

The prepared zein nanoparticle dispersions were centrifuged at 15,000 rpm for 50 min to remove the free drug. Then the free drug was diluted by 0.1 N hydrochloride solution and determined using ultraviolet spectrophotometer at λ_{max} 266 nm. The total drugs in nanoparticles were determined by the following method. One milliliter ZPs dispersion was dissolved by 0.1 N NaOH solution, then 0.1 N HCl solution was added to aggregate zein. The solution was filtered through 0.22 μm filters and assayed spectrophotometrically. Drug encapsulation efficiency and loading were determined by following equations respectively.

$$\text{Drug loading efficiency (\%, w/w)} = \frac{\text{Mass of drug in nanoparticles}}{\text{Mass of nanoparticles}} \times 100$$

$$\text{Drug encapsulation efficiency (\%, w/w)} = \frac{\text{Mass of drug in nanoparticles}}{\text{Mass of feed drug}} \times 100$$

2.4. Optimization of the formulation

The optimization was applied to determine the encapsulated efficiency of the drug. The uniform experimental design U_{10} (10^5) was used (Table 1). The five factors were the ratio of the polymer and 5-FU (v/v) (X_1), zein concentration (mg/ml) (X_2), pH (X_3), stirring time (h) (X_4) and ethanol concentration (%) (X_5).

2.5. Physical properties of the ZPs

The morphology of the nanoparticles was observed by field transmission electron microscopy (TEM) (JEM-1200EX, Japan). A drop of diluted nanoparticles suspension was placed on a 400 mesh carbon-coated copper grid. After drying, the samples were dyed using 2% sodium phosphotungstate.

The particle size and size distribution of drug-loaded ZPs were elucidated by ZETASIZER (3000, Malvern, U.K.). For a better measurement the ZPs suspension was diluted with deionized water to a favorable concentration. The average of hydrodynamic particle size was expressed as the value of *z*-average size ± S.D. from three replicate samples.

Drug-loaded ZPs suspension was diluted with deionized water to ensure that the signal intensity is suitable for the instrument. The zeta potential was measured with laser Doppler velocimetry (DXD-II, Jiangsu, China) at 26 V. Values are presented as mean ± S.D. from three replicate samples.

2.6. Differential scanning calorimetry (DSC)

The physical state of 5-FU inside the ZPs was investigated by differential scanning calorimetry (Shimadzu DSC-41, Japan). The samples were purged with dry nitrogen at a flow rate of 20 ml/min. The temperature was raised at 10 °C/min.

Table 2
The results of uniform experimental design.

Formulation	X_1	X_2 (mg/ml)	X_3	X_4 (h)	X_5 (%)	Encapsulation efficiency (%)	Drug load (%)
1	8:1	2.5	4.0	4	45	6.87	0.76
2	12:1	7.5	9.18	2	45	29.0	1.92
3	2:1	5.0	7.8	1	35	27.3	6.19
4	8:1	12.5	4.0	1	30	19.8	0.86
5	12:1	2.5	5.8	2	25	14.8	0.48
6	4:1	7.5	3.0	5	30	23.4	4.22
7	2:1	12.5	5.8	4	40	44.7	7.13
8	16:1	10.0	3.0	3	40	19.3	0.66
9	16:1	5.0	7.8	5	35	8.83	0.52
10	4:1	10.0	9.18	3	25	56.7	9.05

2.7. In vitro drug release

The in vitro drug release tests were determined by dialysis method. As regards to sink condition, 12.5 mg 5-FU-loaded ZPs was placed into the dialysis bag and carried out using the USP dissolution apparatus (UV2102 PCS, UNICO, Shanghai) fixed with rotating baskets. The dissolution medium was USP phosphate buffer, pH 6.8 and pH 7.4 (200 ml, 37 °C) respectively, and the speed of rotation was 100 rpm. Samples of 5 ml were withdrawn with media replacement at regular intervals, filtered through 0.45 μm filters and assayed for 5-FU at its λ_{max} 266 nm. Each dissolution study was carried out in triplicate.

2.8. Stability studies of the formulations

The physical stability of the ZPs suspension was evaluated after storing them for 6 months under different temperature conditions. Exact volumes of each ZPs suspension were stored in closed glass bottles and placed at 4 °C, 20 °C, and 40 °C respectively. Aliquots of 2 ml were withdrawn to determine drug leakage.

2.9. Biodistribution and blood residence in vivo

The mice were used in vivo study according to national guideline. The experiments have been approved under the institutional ethics committee. The ZPs was labeled with rhodamine B. The mice, with a body weight between 20 ± 1 g, were used for biodistribution and blood residence investigations. The mice were fasted overnight but had free access to water. A total of 60 mice were used in this study. The mice were randomly assigned to two groups and injected intravenously through the tail vein with rhodamine-B solution and rhodamine-B ZPs respectively. The dose was injected intravenously corresponding to 15 mg/kg (body weight of mice). After injection for predetermined time (5 min, 15 min, 30 min, 1 h, 2 h, 4 h, 6 h, 8 h, 12 h and 24 h) the mice were sacrificed. The three parallel mice were used for study at each time point (n = 3). The organs (heart, lung, liver, spleen, and kidney) were exercised, washed by isotonic saline and were rapidly frozen at −20 °C. Blood samples were collected at predetermined time intervals after injection in mice.

Biodistribution and blood residence of particles was determined by measuring the fluorescence of rhodamine B after extraction from the particles in blood or organs into methanol–water (50:50 (v/v)). The extractions were carried out as follows. Blood samples (0.1 ml) were added into 1.9 ml methanol–water containing 0.3 mol/L HCl, and then mixing 2 min and centrifugation (10,000 rpm/min) for 20 min, the supernatant liquid was taken for fluorescence analysis. Organs samples were homogenized with 1–2 ml of physiological saline, then carried out as similar procedure as the above blood samples. The concentration of rhodamine B was assayed on a fluorescence spectroscopy (F-4500, Hitachi, Japan) using λ_{ex} = 554 nm and λ_{em} = 574 nm. The percent cumulative amount in organs and in blood can be calculated. Three mice were intravenously injected for each sampling point.

2.10. Evaluation of targeting efficiency

The target efficiency in vivo was evaluated with T_e, relative uptake rate (r_e) and peak concentration rate C_e. $T_e = AUC_{target}/AUC_{total}$, $r_e = AUC_p/AUC_s$, $C_e = (C_{max})_p/(C_{max})_s$; s and p are rhodamine B solution and ZPs respectively.

2.11. Statistical analysis

Statistical analysis for the determination of differences in the animal study between groups was accomplished with t-test. All data are presented as a mean value with its standard deviation indicated (mean ± S.D.). Differences were considered to be significant at a level of $p < 0.05$.

3. Results and discussion

3.1. Optimization of the formulation

The results of uniform experimental design are shown in Table 2. The optimized formulation was determined as: zein: 5-FU, 3:1 (v/v); zein concentration, 12.5 mg/ml; pH 9.18; stirring time, 3 h and ethanol concentration, 40%. From regression equation, the optimized encapsulation range of above conditions was 66.99 ± 8.27%. In order to validate it, three parallel tests were performed using the optimized preparation conditions. The encapsulation efficiency and the drug loading were 60.7 ± 1.74% and 9.17 ± 0.11% respectively.

Zein is characterized by a high content of charged amino acids. At basic pH, the size of the protein aggregates as well as the void spaces within a particle generally decreases. In addition, proteins are generally more unfolded at basic pH which exposes more reactive sites for cross-linking. Therefore, the encapsulation efficiency of 5-FU was higher than another study in literature, where zein was used to encapsulate Gitoxin (Muthuselvi and Dhathathreyan, 2006). The unfolding of the zein molecule at basic pH increases thiol–disulfide interchange reaction, which may enhance particle formation but inhibit the formation of large aggregates.

3.2. Characterization of the optimal nanoparticle formulation

Transmission microscopy showed ZPs with a spherical shape and a smooth surface (Fig. 1). The 5-FU-loaded ZPs do not differ from the unloaded ones. Fig. 2 shows the distribution of 5-FU ZPs formed. The peak was analyzed by intensity. The average diameter and the zeta potential for 5-FU loaded ZPs were 114.9 ± 59.4 nm and −45.75 ± 0.3 mV (n = 3) respectively. The particles with the size around 100 nm accounted for 86% of the total particles, while the larger particles (≥200 nm) accounted for only 14%. The most parti-

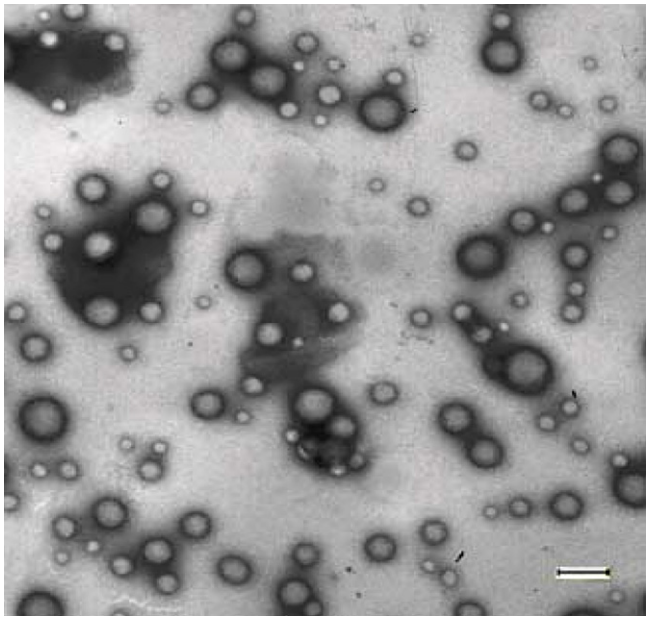

Fig. 1. The TEM image of 5-FU-loaded ZPs (scale bar 0.2 μm).

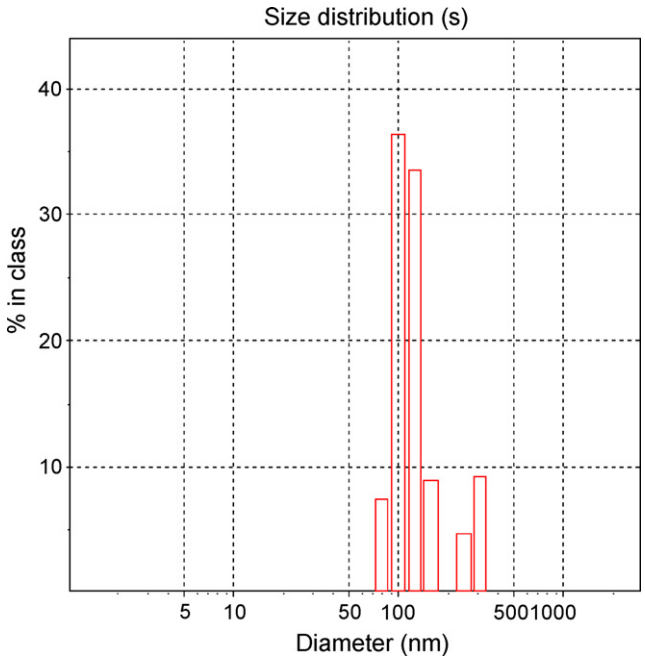

Fig. 2. Size distribution of 5-FU-loaded ZPs.

cles were between 100.5 and 126.5 nm. Zein is characterized by a high content of charged amino acids. At basic pH, the size of the protein aggregates as well as the void spaces within a particle generally decreases. In addition, proteins are generally more unfolded at basic pH which exposes more reactive sites for cross-linking. The unfolding of the zein molecule at basic pH increases thiol–disulfide interchange reaction, which may enhance particle formation but inhibit the formation of large aggregates. The 5-FU nanoparticles prepared at pH 9 were resulted in small zein particles charged negatively on their surface since coacervate precipitation was suppressed at pH 9.0. The magnitude of the zeta potential gives an indication of the potential stability of the colloidal system. Nanoparticles with a zeta potential above ±30 mV have been shown to be stable in suspension, as the surface charge prevents aggregation of the particles. The ZPs with zeta potentials −45.75 mV are normally considered stable.

3.3. Differential scanning calorimetry (DSC)

The DSC thermograms corresponding to 5-FU, zein, physical mixture and 5-FU ZPs are shown in Fig. 3. The DSC curve of 5-FU

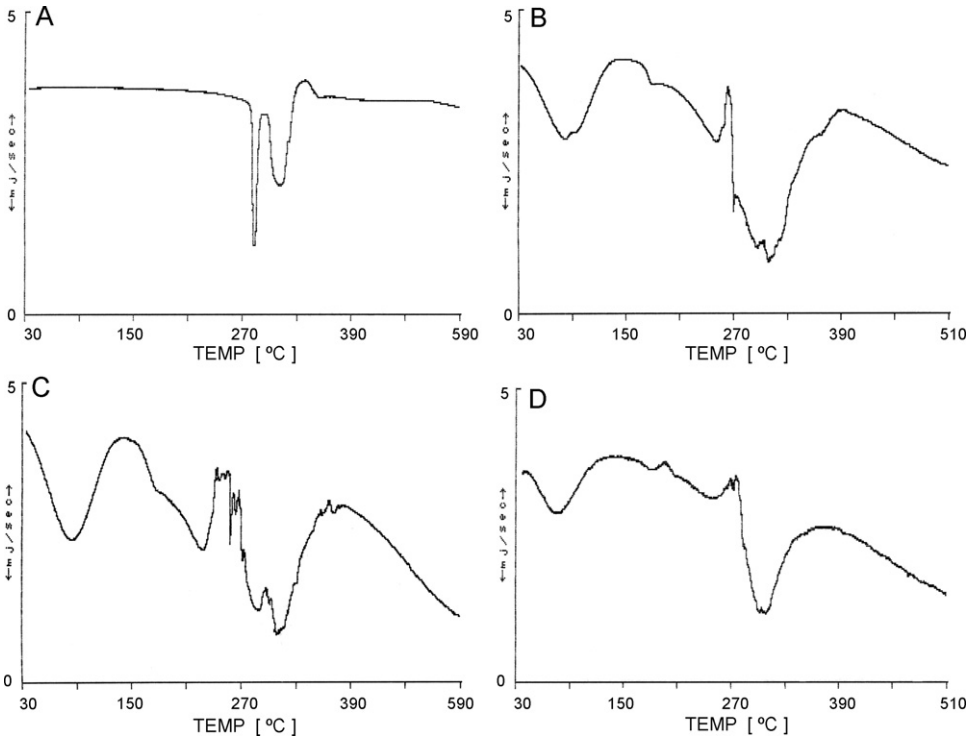

Fig. 3. DSC thermograms of 5-FU (A), pure zein (B), physical mixture of 5-FU, zein (C), and 5-FU-loaded ZPs (D).

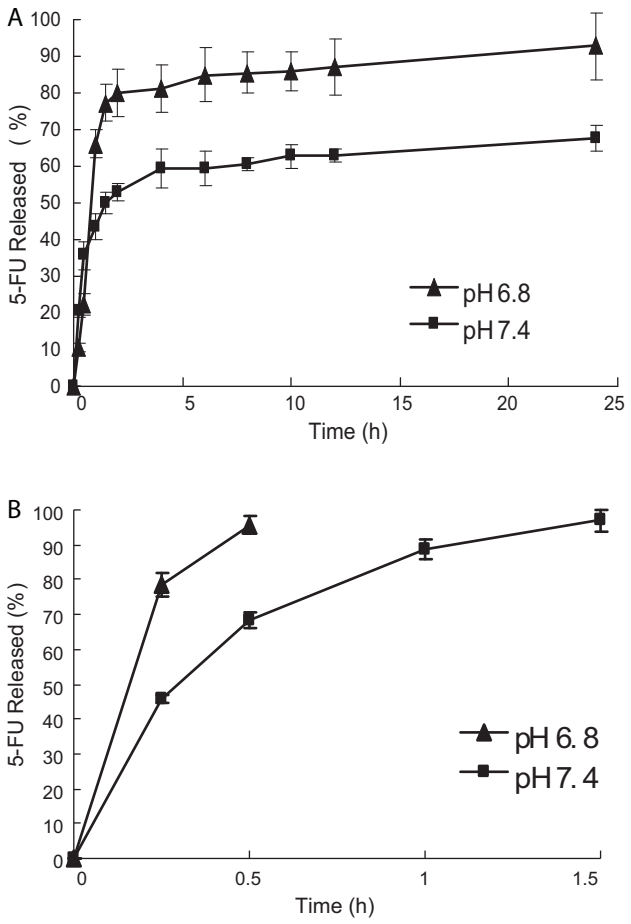

Fig. 4. In vitro release profiles of 5-FU in phosphate buffer pH 6.8 and pH 7.4 from 5-FU-loaded ZPs (A) and 5-FU solution (B) ($n = 3$).

showed a single melting peak at 284.1 °C (Fig. 3A). The zein thermogram displayed an endothermic peak at 309.6 °C (Fig. 3B). For physical mixture the peak was detectable at the melting point of 5-FU (Fig. 3C). However, no characteristic peak of 5-FU was observed in DSC of drug-loaded ZPs, but it showed that the small peak was at 196.9 °C. This suggests that the drug was molecularly dispersed in the polymer matrix (Fig. 3D). There is no detectable endotherm if the drug is present in a molecular dispersion or solid solution state in the polymer systems loaded with drug (Mu and Feng, 2001). The reduction of height and sharpness of the endotherm peak is due to the presence of polymers in the nanoparticles. Since there was no shift in the T_g of the polymer, it can be concluded that there is no significant reaction occurring between the drug and the polymer.

3.4. In vitro drug release of 5-FU-loaded ZPs

In vitro release of 5-FU-loaded ZPs was performed under the pH 6.8 and pH 7.4 phosphate buffer respectively (Fig. 4A). The release rates were different in pH 6.8 and in physiological pH 7.4. A controlled release profile was observed from 5-FU-loaded ZPs. More 5-FU was released in pH 6.8 buffer solution than in pH 7.4 buffer solution. It is because of the solubility of 5-FU in pH 6.8 medium was higher than in pH 7.4 medium (Fig. 4B). Oppositely, the burst release of 5-FU was less in pH 6.8 phosphate buffer solution (22.4%) than in pH 7.4 (35.7%) solution after half hour dissolution. The isoelectric point (pl) of zein is 6.8. The zein's pl can affect its solubility at a pH

Table 3
The encapsulation efficiency and loading of 5-FU in ZPs at different storage temperatures and time.

Time (day)	Temperature		
	4 °C	20 °C	40 °C
0	60.5 ± 1.3	60.5 ± 1.3	60.5 ± 1.3
	10.2 ± 0.56	10.2 ± 0.56	10.2 ± 0.56
10	55.3 ± 1.1	53.6 ± 1.6	32.3 ± 1.5
	9.85 ± 0.49	9.77 ± 0.51	5.6 ± 0.37
30	53.2 ± 0.8	51.6 ± 1.5	
	9.78 ± 0.52	9.65 ± 0.58	–
90	47.8 ± 0.6	45.9 ± 0.8	
	9.25 ± 0.57	8.52 ± 0.46	–
180	45.3 ± 2.5		
	9.02 ± 0.78	–	–

6.8 medium. Zein has minimum solubility at the pH 6.8 medium which corresponds to its pl, which resulted in slower burst release of drug than in pH 7.4 buffer solution. The initial burst release is one of the major problems in the development of controlled release formulations including drug-loaded micro and nanoparticles, especially with low molecular weight drugs (Hasan et al., 2007). The rapid initial release is mainly attributed to weakly bound or adsorbed drug to the relatively larger surface of nanoparticles (Magenheim et al., 1993).

3.5. Stability of 5-FU-loaded ZPs

The 5-FU loaded ZPs suspension stored at 4 °C, 25 °C, and 40 °C respectively. The drug loading and encapsulation efficiency decreased sharply at 40 °C after 10 days (Table 3). On the contrary, at 4 °C or at 25 °C, the drug loading and encapsulation efficiency decreased slowly during the test time. However, the ZPs at 25 °C were aggregated after 6 months storage, while at 4 °C the ZPs were not. Moreover, at 4 °C the encapsulation efficiency and drug loading of ZPs decreased less than the other storage conditions (25 °C and 40 °C). The drug loading decreased only 1% after 6 months storage at 4 °C. Therefore, the ZPs were suitable to be stored at 4 °C. This is reasonable because zein is a hydrophobic corn protein. Generally, proteins are best stored at ≤4 °C. Storage at room or higher temperature often leads to protein degradation and/or inactivity.

3.6. Biodistribution and target efficiency in vivo

The rhodamine B is soluble in water and ethanol. Therefore it could be possible as a fluorescence marker to encapsulate it into ZPs. The distribution profile of the ZPs in organs following intravenous administration in the mice is shown in Fig. 5. It is evident from Fig. 5A and B that the accumulation of fluorescent signals differed significantly between the rhodamine B solution and ZPs in liver, kidney and blood. A rapid elimination from the blood stream was observed for rhodamine B solution after 12 h. At 2 h, the extent of relative distribution from ZPs was higher for the liver (56.7%), followed by the plasma (20.8%), spleen (7.3%), kidney (6.7%), lung (4.3%) and heart (4.1%). The relative percentage of fluorescent signals from ZPs attained a maximum value of 63.6 ± 0.79% in the livers at the time point of 24 h. In contrast, there was no fluorescence detected for the rhodamine B solution accumulation at 24 h after administration. The statistical significance between two groups was in liver, kidney, spleen and heart, however there was no significant difference in lung and blood during 6 h and 12 h period.

The targeting efficiency of rhodamine B after administration of rhodamine B solution and ZPs was shown in Table 4. Highly fluorescent intensity was observed in the liver; there was a distinct difference ($p < 0.001$) between the rhodamine B solution and the ZPs. The results revealed that the ZPs were mostly accumulated

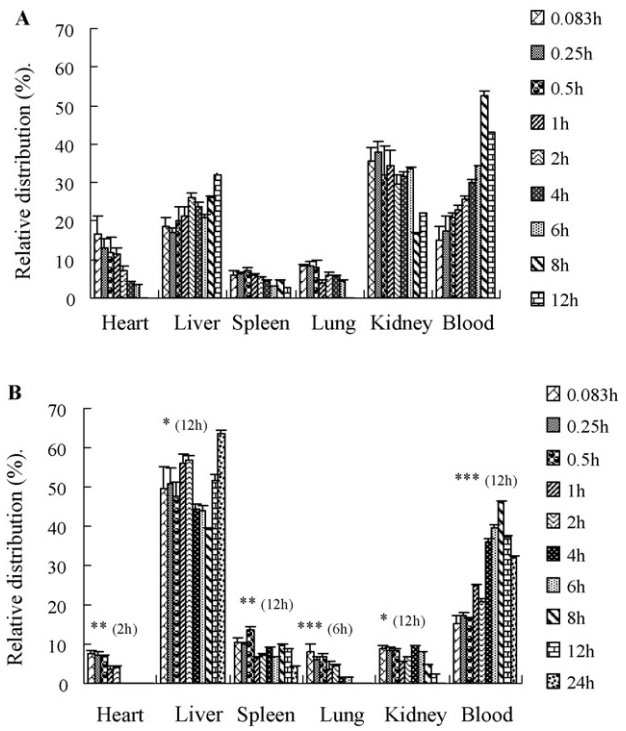

Fig. 5. Relative fluorescence distribution in tissues and blood after intravenous administration of rhodamine B solution (A) and ZPs (B) to mice respectively. Data were given as mean ± S.D. ($n = 3$). Statistical significance compared between two groups: $^{*}p < 0.001$, $^{**}p < 0.05$ and $^{***}p > 0.05$.

as the highest fluorescent intensity in the liver. Even at 24 h after the parenteral delivery of the ZPs, there were no fluorescence signals in other organs. Moreover, the targeting efficiency increased 31.33%. The fluorescence intensity of ZPs in the livers increased 2.13 times compared to the rhodamine B solution. The relative uptake rate of liver was 2.79, indicating that the ZPs was specific to the liver tissue. The relative uptake rate of ZPs was in the order of liver > spleen > plasma > lung > heart > kidney. The accumulation of fluorescent signals was the highest for the liver and the lowest for the kidney. The relative higher fluorescence intensity observed for rhodamine B solution in the kidneys than ZPs, suggesting that the rhodamine B was mainly eliminated from the kidney, and thus accumulation increased in the kidneys.

Passive delivery may also be directed to lymphoid organs of the mammalian immune system, such as lymphatic vessels and spleen. These organs are finely structured and specialized in eliminating invaders that have gained entry to tissue fluids. Nanoparticles may easily penetrate into lymphatic vessels, taking advantage of the thin walls and fenestrated architecture of lymphatic microvessels. Passive targeting to the spleen is via a process of filtration. The spleen filters the blood of foreign particles larger than 200 nm (Moghimi, 1995). In our case, the average size of ZPs was smaller than 200 nm.

Table 4
Targeting efficiency after intravenous administration of rhodamine B solution and ZPs ($n = 3$).

Tissue and plasma	Rhodamine B solution	Rhodamine B-loaded ZPs		
	T_e (%)	T_e (%)	r_e	C_e
Heart	7.82	2.25	0.34	0.37
Liver	22.67	54.00	2.79	2.13
Spleen	5.23	8.68	1.94	1.38
Lung	5.18	3.08	0.70	0.79
Kidney	31.88	6.56	0.24	0.20
Plasma	27.22	25.43	1.09	0.86

Thus, smaller particle size of ZPs resulted in relatively high distribution percentage in the spleen. In the liver, the fenestrae-associated cytoskeleton controls the hepatic function of endothelial filtration, where the size of fenestrae can be as large as 150 nm (Braet et al., 1995). The size of fenestrae in certain inflammatory vessels as well as tumor capillaries can be up to 700 nm. Polymeric nanospheres (in the range of 50–200 nm) could increase capillary permeability during inflammation (Dams et al., 1998) and in specific cancers (Poznansky and Juliano, 1984; Hobbs et al., 1998) based on observations in experimental animals and in humans. Thus, large particles hardly reach the liver's parenchymal cells. Additionally, drug carriers with a diameter larger than 200 nm are readily scavenged non-specifically by monocytes and the reticuloendothelial system (RES) (Litzinger et al., 1994). It was reported that smaller particles tended to be accumulated at the tumor sites because of the EPR effect (Maeda and Matsumura, 1989); greater internalization was also observed (Li, 2002). Therefore, the optimized average size of ZPs (114.9 nm) could be targeted to liver tumor via EPR effect.

Applications of nanoparticles are limited by their rapid recognition by the RES. In fact, they are cleared from the bloodstream within minutes upon intravenous injection, depending on their size and surface characteristics (Moghimi et al., 2001; Verdun et al., 1990; Moghimi and Szebeni, 2003). In our study, even at 24 h after the parenteral delivery of the ZPs, the accumulation of fluorescent signal was the highest in the liver, and the fluorescence intensity in blood was still observed at 24 h. It showed that ZPs were not rapidly cleared from blood. It seemed that ZPs upon intravenous injection avoided rapid recognition by Kupffer cells and adequately remained in the blood. It was reported that the areas under the concentration curve vs. time (AUC) of a drug and its tumor uptake are positively related, whereas the rate of urinary clearance is inversely related to tumor uptake (Matsumura and Maeda, 1986; Maeda et al., 2001; Noguchi et al., 1998; Seymour et al., 1994). The higher AUC and lower renal excretion was observed in rhodamine B labeled ZPs than rhodamine B solution. Therefore, the drug encapsulated in ZPs could be efficient targeted to liver's parenchymal cells via passive delivery.

4. Conclusions

The drug-loaded (e.g. 5-FU) ZPs could be prepared and optimized for liver targeting. The higher encapsulation efficiency and drug loading could be achieved using uniform experimental design. DSC study indicates 5-FU was encapsulated in the ZPs. In vitro drug release of 5-FU-loaded ZPs revealed a sustained release profile. The 5-FU-loaded ZPs are more stable at 4 °C than at higher temperature (e.g. 25 °C and 40 °C). The ZPs distributed mostly in liver after intravenous administration to mice and adequately remained in the blood for at least 24 h due to its relatively higher molecular weight and smaller particle size. This study demonstrated that the drug-loaded ZPs could be efficiently targeted at the liver by intravenous delivery.

References

Braet, F., Dezanger, R., Baekeland, M., Crabbe, E., van der Smissen, P., Wisse, E., 1995. Structure and dynamics of the fenestrae-associated cytoskeleton of rat-liver sinusoidal endothelial cells. Hepatology 21, 180–189.

Couvreur, P., Kante, B., Lenaerts, V., Scailteur, V., Roland, M., Speiser, P., 1980. Tissue distribution of antitumor drugs associated delivery of encapsulated dextran–doxorubicin conjugate with polyalkylcyanoacrylate nanoparticles. J. Pharm. Sci. 69, 199–202.

Dams, E.T.M., Oyen, W.J.G., Boerman, O.C., Storm, G., Laverman, P., Koenders, E.B., et al., 1998. Technetium-99m-labeled liposomes to image experimental colitis in rabbits: comparison with technetium-99m-HMPAOgranulocytes and technetium-99m-HYNIC-IgG. J. Nucl. Med. 39, 2172–2178.

Dong, J., Sun, Q.Sh., Wang, J.Y., 2004. Basic study of corn protein, zein, as a biomaterial in tissue engineering, surface morphology and biocompatibility. Biomaterials 25, 4691–4697.

Greenman, C., Stephens, P., Smith, R., Dalgliesh, G.L., Hunter, C., Bignell, G., Davies, H., Teague, J., Butler, A., Stevens, C., Edkins, S., O'Meara, S., Vastrik, I., Schmidt, E.E., Avis, T., et al., 2007. Patterns of somatic mutation in human cancer genomes. Nature 446, 153–158.

Gref, R., Minamitake, Y., Peracchia, M.T., Trubetskoy, V., Torchilin, V., Langer, R., 1994. Biodegradable long-circulating polymeric nanospheres. Science 263, 1600–1603.

Grem, J.L., 1990. Fluorinated pyrimidines. In: Chabner, B.A., Collins, J.M. (Eds.), Cancer Chemotherapy: Principles and Practice. J.B. Lippincott Company, Philadelphia, PA, pp. 180–224.

Guo, Y., Liu, Z., An, H., Li, M., Hu, J., 2005. Nano-structure and properties of maize zein studied by atomic force microscopy. J. Cereal Sci. 41, 277–281.

Hasan, A.S., Socha, M., Lamprecht, A., Ghazouani, F.E., Sapin, A., Hoffman, M., Maincent, P., Ubrich, N., 2007. Effect of the microencapsulation of nanoparticles on the reduction of burst release. Int. J. Pharm. 344, 53–61.

Hobbs, S.K., Monsky, W.L., Yuan, F., Roberts, W.G., Griffith, L., Torchilin, V.P., et al., 1998. Regulation of transport pathways in tumor vessels: role of tumor type and microenvironment. Proc. Natl. Acad. Sci. U.S.A. 95, 4607–4612.

Lamprecht, A., Yamamoto, H., Takeuchi, H., Kawashima, Y., 2003. Microsphere design for the colonic delivery of 5-fluorouracil. J. Control. Release 90, 313–322.

Li, C., 2002. Poly(L-glutamic acid)-anticancer drug conjugates. Adv. Drug Deliv. Rev. 54, 695–713.

Litzinger, D.C., Buiting, A.M.J., Rooijen, N., Huang, L., 1994. Effect of liposome size on the circulation time and intraorgan distribution of amphipathic poly(ethylene glycol)-containing liposomes. Biochim. Biophys. Acta 1190, 99–107.

Liu, X., Sun, Q., Wang, H., Zhang, L., Wang, J., 2005. Microspheres of corn protein, zein, for an ivermectin drug delivery system. Biomaterials 26, 109–115.

Maeda, H., Matsumura, Y., 1989. Tumoritropic and lymphotropic principles of macromolecular drugs. Crit. Rev. Ther. Drug Carrier Syst. 6, 193–210.

Maeda, H., Sawa, T., Konno, T., 2001. Mechanism of tumor-targeted delivery of macromolecular drugs, including the EPR effect in solid tumor and clinical overview of the prototype polymeric drug SMANCS. J. Control. Release 74, 47–61.

Maeda, H., Bharate, G.Y., Daruwalla, J., 2009. Polymeric drugs for efficient tumor-targeted drug delivery based on EPR-effect. Eur. J. Pharm. Biopharm. 71, 409–419.

Magenheim, B., Levy, M.Y., Benita, S., 1993. A new in vitro technique for the evaluation of drug release profile from colloidal carriers—ultrafiltration technique at low pressure. Int. J. Pharm. 94, 115–123.

Matsumura, Y., Maeda, H., 1986. A new concept for macromolecular therapeutics in cancer chemotherapy: mechanism of tumoritropic accumulation of proteins and the antitumor agent smancs. Cancer Res. 46, 6387–6392.

McClean, S., Prosser, E., Meehan, E., O'Malley, D., Clarke, N., Ramtoola, Z., et al., 1998. Binding and uptake of biodegradable poly-lactide micro- and nanoparticles in intestinal epithelia. Eur. J. Pharm. Sci. 6, 153–163.

Moghimi, S.M., 1995. Mechanisms of splenic clearance of blood cells and particles: towards development of new splenotropic agents. Adv. Drug Deliv. Rev. 17, 103–115.

Moghimi, S.M., Hunter, A.C., Murray, J.C., 2001. Long-circulating and target-specific nanoparticles: theory to practice. Pharmacol. Rev. 53, 283–318.

Moghimi, S.M., Szebeni, J., 2003. Stealth liposomes and long circulating nanoparticles: critical issues in pharmacokinetics, opsonization and protein-binding properties. Prog. Lipid Res. 42, 463–478.

Mu, L., Feng, S.S., 2001. Fabrication characterization and in vitro release of paclitaxel (Taxol) loaded poly (lactic-*co*-glycolic acid) microspheres prepared by spray drying technique with lipid/cholesterol emulsifiers. J. Control. Release 76, 239–254.

Muthuselvi, L., Dhathathreyan, A., 2006. Simple coacervates of zein to encapsulate Gitoxin. Colloids Surf. B: Biointerfaces 51, 39–43.

Noguchi, Y., Wu, J., Duncan, R., Strohalm, J., Ulbrich, K., Akaike, T., et al., 1998. Early phase tumor accumulation of macromolecules: a great difference in clearance rate between tumor and normal tissues. Jpn. J. Cancer Res. 89, 307–314.

Park, T.G., Lu, W.Q., Crotts, G., 1995. Importance of in vitro experimental conditions on protein release kinetics, stability and polymer degradation in protein encapsulated poly(D, L-lactic acid-co-glycolic acid) microspheres. J. Control. Release 33, 211–222.

Poznansky, M., Juliano, R.L., 1984. Biological approaches to the controlled delivery of drugs: a critical review. Pharmacol. Rev. 36, 277–336.

Seymour, L.W., Ulbrich, K., Steyger, P.S., Brereton, M., Subr, V., Strohalm, J., et al., 1994. Tumor tropism and anti-cancer efficacy of polymer-based doxorubicin prodrugs in the treatment of subcutaneous murine B16F10 melanoma. Br. J. Cancer 70, 636–641.

Sledge, G.W., Miller, K.D., 2003. Exploiting the hallmarks of cancer: the future conquest of breast cancer. Eur. J. Cancer 39, 1668–1675.

Soppimath, K.S., Aminabhavi, T.M., Kulkarni, A.R., Rudzinski, W.E., 2001. Biodegradable polymeric nanoparticles as drug delivery devices. J. Control. Release 70, 1–20.

Tanaka, F., Fukuse, T., Wada, H., Fukushima, M., 2000. The history, mechanism and clinical use of oral 5-fluorouracil derivative chemotherapeutic agents. Curr. Pharm. Biotech. 1, 137–164.

Teicher, B.A., 2000. Molecular targets and cancer therapeutics: discovery, development and clinical validation. Drug Resist. Updat. 3, 67–73.

Tobias, S., Sian, J., Laura, D., Wood, D., Parsons, W., 2006. The consensus coding sequences of human breast and colorectal cancers. Science 314, 268–274.

Wang, H.J., Lin, Z.X., Liu, X.M., Sheng, S.Y., Wang, J.Y., 2005. Heparin-loaded zein microsphere film and hemocompatibility. J. Control. Release 105, 120–131.

Wang, H.J., Gong, S.J., Lin, Z.X., Fu, J.X., Xue, S.T., Huang, J.C., Wang, J.Y., 2007. In vivo biocompatibility and mechanical properties of porous zein scaffolds. Biomaterials 20, 3952–3964.

Verdun, C., Brasseur, F., Vranckx, H., Couvreur, P., Roland, M., 1990. Tissue distribution of doxorubicin associated with polyisohexylcyanoacrylate nanoparticles. Cancer Chemother. Pharmacol. 26, 13–18.

Yuan, F., 1998. Transvascular drug delivery in solid tumors. Semin. Radiat. Oncol. 8, 164–175.

Zan, J., Zhu, D., Tan, F., Jiang, G., Lin, Y., Ding, F., 2006. Preparation of thermosensitive chitosan formulations containing 5-fluorouracil/poly-3-hydroxybutyrate microparticles used as injectable drug delivery system. Chin. J. Chem. Eng. 14, 235–241.